ADVANCES IN ATMOSPHERIC SCIENCES, VOL. 30, NO. 1, 2013, 57–66

Enhancements of Major Aerosol Components Due to Additional HONO Sources in the North China Plain and Implications for Visibility and Haze

AN Junling*[1] (安俊岭), LI Ying[1,2] (李 颖), CHEN Yong[1] (陈 勇), LI Jian[1,2] (李 健), QU Yu[1] (屈 玉), and TANG Yujia[1,2] (汤宇佳)

[1] *State Key Laboratory of Atmospheric Boundary Layer Physics and Atmospheric Chemistry, Institute of Atmospheric Physics, Chinese Academy of Sciences, Beijing* 100029

[2] *University of Chinese Academy of Sciences, Beijing* 100049

(Received 17 January 2012; revised 10 May 2012)

ABSTRACT

The Weather Research and Forecasting/Chemistry model (WRF-Chem) was updated by including photoexcited nitrogen dioxide (NO_2) molecules, heterogeneous reactions on aerosol surfaces, and direct emissions of nitrous acid (HONO) in the Carbon-Bond Mechanism Z (CBM-Z). Five simulations were conducted to assess the effects of each new component and the three additional HONO sources on concentrations of major chemical components. We calculated percentage changes of major aerosol components and concentration ratios of gas NO_y (NO_{yg}) to NO_y and particulate nitrates (NO_3^-) to NO_y due to the three additional HONO sources in the North China Plain in August of 2007. Our results indicate that when the three additional HONO sources are included, WRF-Chem can reasonably reproduce the HONO observations. Heterogeneous reactions on aerosol surfaces are a key contributor to concentrations of HONO, nitrates (NO_3^-), ammonium (NH_4^+), and $PM_{2.5}$ (concentration of particulate matter of $\leqslant$2.5 μm in the ambient air) across the North China Plain. The three additional HONO sources produced a ∼5%–20% increase in monthly mean daytime concentration ratios of NO_3^-/NO_y, a ∼15%–52% increase in maximum hourly mean concentration ratios of NO_3^-/NO_y, and a ∼10%–50% increase in monthly mean concentrations of NO_3^- and NH_4^+ across large areas of the North China Plain. For the Bohai Bay, the largest hourly increases of NO_3^- exceeded 90%, of NH_4^+ exceeded 80%, and of $PM_{2.5}$ exceeded 40%, due to the three additional HONO sources. This implies that the three additional HONO sources can aggravate regional air pollution, further impair visibility, and enhance the incidence of haze in some industrialized regions with high emissions of NO_x and particulate matter under favorable meteorological conditions.

Key words: HONO, NO_y, aerosol component, heterogeneous reaction, WRF-Chem model

Citation: An, J. L., Y. Li, Y. Chen, J. Li, Y. Qu, and Y. J. Tang, 2013: Enhancements of major aerosol components due to additional HONO sources in the North China Plain and implications for visibility and haze. *Adv. Atmos. Sci.*, **30**(1), 57–66, doi: 10.1007/s00376-012-2016-9.

1. Introduction

Nitrous acid (HONO) is one of the major sources of the hydroxyl radical (OH), which is the key oxidant in the atmosphere. Direct emissions, gas-phase reactions, and heterogeneous reactions are generally considered as HONO sources, but the detailed formation mechanism of HONO is still under discussion. High HONO concentrations in urban or rural areas are frequently observed (Su et al., 2008; An et al., 2009; Qin et al., 2009; Yu et al., 2009), but most current air-quality models, such as WRF-Chem, cannot reproduce HONO observations very well, particularly in the daytime, due mainly to the only inclusion of gas-phase production of HONO (Li et al., 2010; An et al., 2011; Li et al., 2011). Recently, Sarwar et al. (2008) added HONO emissions by using the $HONO/NO_x$ emission ratio of 0.8%, $2NO_2 + H_2O +$ aerosol/ground surfaces $\rightarrow$ HONO

*Corresponding author: AN Junling, anjl@mail.iap.ac.cn

+ HNO_3, and HNO_3 (adsorbed) + $h\nu \rightarrow$ 0.5HONO (adsorbed) + 0.5NO_2 (adsorbed) into the Community Multiscale Air Quality model (CMAQ) (Foley et al., 2009). HONO simulations were improved, but obvious discrepancies between simulated and observed HONO concentrations still existed in the daytime period (Sarwar et al., 2008). Li et al. (2008) proposed a new production mechanism of HONO through photoexcited NO_2 chemistry (R_{NO2S}, where S means photoexcited). The importance of R_{NO2S} is still argued (Crowley and Carl, 1997; Wennberg and Dabdub, 2008; Sarwar et al., 2009; Ensberg et al., 2010; An et al., 2011; Li et al., 2011). For heterogeneous reactions, Li et al. (2010) considered both aerosol and ground surface reactions in WRF-Chem; however, field experiments showed a good correlation between concentrations of particulate matter and HONO (An et al., 2009), or between aerosol surface area and HONO concentrations (Ziemba et al., 2010), suggesting that aerosol surface is the dominant reaction substrate and that stationary sources (e.g., buildings and soils) are likely insignificant (Ziemba et al., 2010). Additionally, Li et al. (2010) used a relatively high emission ratio of 2.3% for HONO/NO_2 to calculate direct emissions of HONO. This could lead to overestimation of HONO concentrations in the air. Recently, Su et al. (2011) have suggested that soil nitrites are a source of HONO emissions, but nitrite concentrations in soils are generally low (Cleemput and Samater, 1996), and related field observations are scarce. Based on the current understanding of HONO sources, An et al. (2011) and Li et al. (2011) incorporated heterogeneous reactions on aerosol surfaces (R_{het}), an improved parameterization scheme (see section 2.2) for direct emissions of HONO (R_{em}), and R_{NO2S}, which could be important in areas where NO_x emissions are elevated (e.g., the North China Plain), into WRF-Chem and found that the three additional HONO sources (i.e., R_{NO2S}, R_{het}, and R_{em}) significantly improved HONO simulations in comparison with observations from differential optical absorption spectroscopy (DOAS) (Zhu et al., 2009), particularly in the daytime.

The purpose of this study was to compute the contributions of R_{NO2S}, R_{het}, R_{em}, and the three additional HONO sources (R_{NO2S}, R_{het}, and R_{em}) to concentrations of major chemical components and to estimate percentage enhancements of major aerosol components (i.e., NO_3^-, NH_4^+, SO_4^{2-}, and also $PM_{2.5}$) due to the three additional HONO sources in the North China Plain, where emissions of NO_x and particulate matter (PM) are high (Zhang et al., 2009). Changes were calculated in concentration gas ratios of NO_y (i.e., $NO_{yg} = NO + NO_2 + NO_3 + PAN + HNO_3 + HONO + HNO_4 + N_2O_5$) to NO_y (i.e., $NO_y = NO_{yg} +$ particulate nitrates) and particulate nitrates (NO_3^-) to NO_y due to the three additional HONO sources. The implications of these results were analyzed and were discussed in section 3.

2. Methodology

2.1 *WRF-Chem model setup*

The WRF-Chem version 3.2.1 (Grell et al., 2005; Fast et al., 2006) was utilized in this study. Physical and chemical schemes for simulations followed those of An et al. (2011) and Li et al. (2011). Two nested domains were used in the simulation; domain 3 covered the North China Plain (An et al., 2011; Li et al., 2011). We used 28 vertical model layers from the ground to ∼50 hPa, with the first layer 28 m above the ground. Initial and boundary conditions for meteorological fields were obtained from NCEP reanalysis data applied to nudging every 6 h, and initial and boundary conditions for chemical fields were constrained using the output of the Model for Ozone and Related chemical Tracers,version 4 (MOZART-4) (Emmons et al., 2010) every 6 h. Anthropogenic emissions of sulfur dioxide (SO_2), nitrogen oxides (NO_x), carbon monoxide (CO), volatile organic compounds (VOCs), PM_{10}, $PM_{2.5}$, black carbon (BC), and organic carbon (OC) were taken from Zhang et al. (2009), and those of NH_3 were adopted from Streets et al. (2003). Changes in NH_3 emissions between 2000 and 2006 were insignificant (Zhang et al., 2009). Biogenic emissions were computed on the basis of the work of Guenther et al. (1993) and Simpson et al. (1995). Five model simulations (cases A, B, C, R, and E) were conducted to calculate contributions of each component as well as the three additional HONO sources to concentrations of major chemical components in percentage change concentrations of NO_3^-, NH_4^+, SO_4^{2-}, and $PM_{2.5}$, and concentration ratios of NO_{yg}/NO_y and NO_3^-/NO_y due to the three additional HONO sources in the North China Plain in August 2007. Case R used the Carbon-Bond Mechanism Z (CBM-Z) and the Model for Simulating Aerosol Interactions and Chemistry (MOSAIC) (Zaveri et al., 2008). Cases A, B, C, and E were extensions of case R by inclusion of R_{NO2S}, R_{em}, R_{het}, and the three additional HONO sources ($R_{NO2S} + R_{het} + R_{em}$), respectively (see section 2.2, Table 1).

2.2 *Parameterization of the three additional HONO sources*

For R_{het} ($NO_2 \rightarrow$0.5 HNO_3+ 0.5 HONO), we followed the recommendation of Jacob (2000):

$$k_{het} = S_a \left(\frac{r_p}{D_g} + \frac{4}{u\gamma} \right)^{-1},$$

Table 1. Five simulated scenarios used in this research

Case	Photo-excited NO_2 chemistry	HONO emissions	NO_2 heterogeneous production	Gas-phase production
R				√
A	√			√
B		√		√
C			√	√
E	√	√	√	√

where $k_{\rm het}$ denotes the first-order rate constant and $S_{\rm a}$ is the aerosol surface area per unit volume of air. $S_{\rm a}$ was derived from aerosol mass concentrations and number density in each bin set by the MOSAIC module. Aerosols considered in MOSAIC are composed of sulfate, nitrate, ammonium, chloride, sodium, other inorganics, organic carbon (OC), elemental carbon (EC), and water. $r_{\rm p}$ represents the particle radius (m). $D_{\rm g}$ denotes gas molecular diffusion coefficients estimated as 10^{-5} m^2 s^{-1} (Dentener and Crutzen, 1993). u is the mean molecular speed of NO_2 (m s^{-1}). γ denotes the uptake coefficient of NO_2, taken as 10^{-4} (Jacob, 2000).

HONO emissions ($R_{\rm em}$) were computed using

$$R_{\rm em} = [0.023 \times f_{\rm DV} + 0.008 \times (1 - f_{\rm DV})] \times f_{\rm TS}$$

where $f_{\rm DV}$ stands for the NO_x emission ratio of diesel vehicles to total vehicles. The averaged $f_{\rm DV}$ was 62% in China in 2006 (Li et al., 2011). $f_{\rm TS}$ is the NO_x emission ratio of the traffic source to all anthropogenic sources. The value of 0.8% has been suggested by Kurtenbach et al. (2001) and was used by Aumont et al. (2003), Sarwar et al. (2008), and An et al. (2009). A fraction of 2.3% of the NO_x emitted in diesel exhaust can be heterogeneously converted to HONO (Gutzwiller et al., 2002), and this fraction was utilized in this research. $R_{\rm het}$ and $R_{\rm NO2S}$ were added to the CBM-Z mechanism, as introduced by Li et al. (2011).

3. Results and discussion

3.1 *Comparison of simulations and observations*

HONO concentrations measured by DOAS in Beijing on 13–25 August 2007 were obtained from Zhu et al. (2009). Ozone (O_3), NO_x, and PM_{10} were simultaneously monitored at the 325-m meteorological tower in Beijing (Li et al., 2011). Li et al. (2011) demonstrated good agreement between O_3 and NO_2 measurements from DOAS and the O_3 and NO_2 analyzers in Beijing. The correlation coefficients were 0.97 for O_3 and 0.83 for NO_2. Compared with gas-phase reactions (case R), the inclusion of $R_{\rm het}$, $R_{\rm em}$, and $R_{\rm NO2S}$ in WRF-Chem (case E) led to significant improvements in HONO simulations of measurements at the 325-m meteorological tower in Beijing (Fig. 1a and Table 2). For example, the root mean square error was reduced by ∼50%, and the correlation coefficient improved to 0.97 from 0.19 (Table 2). However, HONO simulations for case E were overestimated by comparison with observations due to overprediction of PM observations (Fig. 1d) and the exclusion of HO_2 heterogeneous reactions on aerosol surfaces. The HO_2 heterogeneous loss on aerosol surfaces (2 $HO_2 \rightarrow H_2O_2$) considered in Li et al. (2011) lowered HONO simulations when Fig. 1a of this study was compared to Fig. 6a in Li et al. (2011). The uncertainty of the heterogeneous uptake coefficient of HO_2 was high (Thornton and Abbatt, 2005), and the reaction of 2 $HO_2 \rightarrow H_2O_2$ was not a source of HONO, so the HO_2 heterogeneous reaction was excluded from this research and will be investigated in the near future. The three HONO sources can improve daytime O_3 simulations, especially the peak concentrations. Daytime mean value of O_3 was enhanced by 2.5 ppb, and the maximum hourly value was enhanced by 21 ppb (35%) at 1200 LST 16 August. NO_2 nighttime simulations improved significantly, with the mean value reduced by 5.4 ppb, mainly due to the heterogeneous reaction on aerosol surfaces (Li et al., 2011). PM_{10} simulations for cases E and R were reasonable in most cases, except for the period 21–25 August (Fig. 1d). For this period, PM_{10} simulations for cases E and R were substantially overestimated (Fig. 1d), and further investigation was needed. The calculated mean nitrate concentration for case R was 20.13 μg m^{-3}, while that for case E was enhanced to 26.94 μg m^{-3} due to the additional HONO sources. NO_3^- peaks were significantly enhanced, similar to the results of Li et al. (2010).

3.2 *Impacts of each and the three additional HONO sources on major gas components*

$R_{\rm NO2S}$ was shown to enhance the monthly mean daytime (∼0700–1900 LST) HONO by a maximum of 60 ppt (Table 3), being lower than 100 ppt in the Eastern and Western United States (Sarwar et al., 2009). $R_{\rm NO2S}$ and photolysis of HONO can produce more OH, which reacts with VOCs to yield more HO_2. More HO_2 can accelerate conversion of NO to NO_2 and result in more O_3 (Table 3). On the other hand, increases

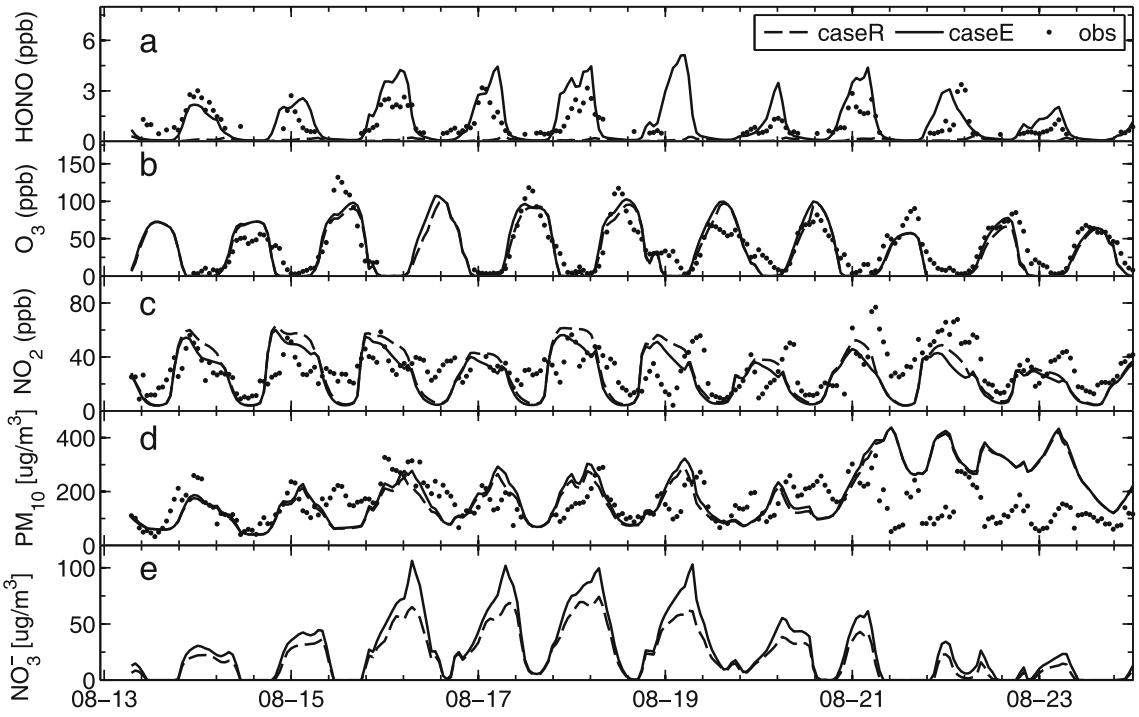

Fig. 1. Comparison of simulated concentrations of (a) HONO, (b) O_3, (c) NO_2, (d) PM_{10}, and (e) NO_3^- for cases E and R with observations from the 325-m meteorological tower in Beijing on 13–25 August 2007. No observations were available for NO_3^-.

in OH can lead to HNO_3 enhancements through the reaction of $NO_2 + OH \rightarrow HNO_3$. The reaction of $HNO_3 + NH_3 \rightarrow NH_4NO_3$ yields noticeable increases of NO_3^- and NH_4^+, with a maximum of 3.0 μg m^{-3} (Table 3). R_{em} produces greater increases of HONO in the nighttime (2000–0600 LST) than in the daytime (Table 3) due to daytime photolysis of HONO. R_{het} plays a pivotal role in the formation of HONO, NO_3^-, NH_4^+ and $PM_{2.5}$ in both daytime and nighttime: R_{het} yielded an increase of 3.4 ppb of maximum monthly mean nighttime HONO, maximum monthly mean daytime NO_3^- was enhanced to 13.3 μg m^{-3} and maximum monthly mean daytime $PM_{2.5}$ was enhanced to 18.1 μg m^{-3} (Table 3). When the three additional HONO sources were considered, the largest increases in monthly mean daytime were 0.6 ppb for HONO, 4.0 ppt for HO_2, 17.0 μg m^{-3} for NO_3^-, 5.5 μg m^{-3} for NH_4^+, and 23.9 μg m^{-3} for $PM_{2.5}$ (Table 3). For O_3 simulations the three additional HONO sources lead to ∼1–20 ppb increases in maximum hourly averages (Fig. 2a) and ∼1–4.9 ppb enhancements of monthly daytime averages (Fig. 2b), with maximum values located areas of elevated emissions in the North China Plain or along the Bohai Bay (see discussion in section 3.3).

3.3 *Impacts of the three additional HONO sources on major aerosol components*

Percent changes in concentrations of air pollutants due to the three additional HONO sources were defined as $(C_E - C_R)\times 100\%/C_R$, where C_E and C_R denote concentrations of air pollutants for cases E and R, respectively. The three additional HONO sources (R_{NO2S}, R_{het}, and R_{em}) resulted in ∼10%–50% enhancements of NO_3^-, ∼10%–40% increases of NH_4^+, ∼6%–15% enhancements of SO_4^{2-}, and ∼3%–12% increase of $PM_{2.5}$ in major cities of the North

Table 2. Model performance statistics for HONO diurnal-averaged simulations of measurements at the 325-m meteorological tower in Beijing on 13–25 August 2007.

Case	Observed mean (ppb)	Simulated mean (ppb)	NMB (%)	RMSE (ppb)	RC
R	1.02	0.08	−92	1.10	0.19
E	1.02	1.12	29	0.66	0.97

Note: NMB, RMSE, and RC denote the normal mean bias, the root mean square error, and the correlation coefficient, respectively.

Table 3. Maximum monthly mean daytime (0700–1900 LST) and nighttime (2000–0600 LST) enhancements of O_3, HONO, OH, HO_2, HNO_3, NO_3^-, NH_4^+, SO_4^{2-}, $PM_{2.5}$, and NO_3^-/NO_y due to photo-excited NO_2 chemistry (case A−case R), direct emissions of HONO (case B−case R), heterogeneous reaction on aerosol surfaces (case C−case R) and the three additional HONO sources (case E−case R). The unit of O_3, HONO, and HNO_3 is ppb, that of OH and HO_2 is ppt, and that of NO_3^-, NH_4^+, SO_4^{2-}, and $PM_{2.5}$ is μg m^{-3}, and that of NO_3^-/NO_y is %. A percentage change is shown in parentheses, and a nighttime enhancement is shown behind a slash and its corresponding percentage change is shown both behind a slash and in parentheses

Species	Case A−case R	Case B−case R	Case C−case R	Case E−case R
O_3	2.0 (4.2)	0.4 (0.9)	3.4 (7.5)	4.9 (11.7)
HONO	0.06 (70.0)	0.09/1.0 (118.4/>200)	0.4/3.4 (>200/>200)	0.6/4.5 (>200/>200)
OH	0.03 (19.4)	0.01 (7.9)	0.09 (55.7)	0.1 (83.6)
HO_2	0.7 (15.6)	0.3 (7.4)	3.2 (59.6)	4.0 (88.9)
HNO_3	0.2 (4.6)	0.02 (0.9)	0.5/0.2 (14.5/40.7)	0.8/0.2 (18.7/40.7)
NO_3^-	3.0 (7.0)	0.4 (1.6)	13.3/13.2 (47.7/47.6)	17.0/14.1 (53.9/51.0)
NH_4^+	1.0 (6.2)	0.1 (1.5)	4.2/3.9 (34.5/35.1)	5.5/4.3 (39.7/38.1)
SO_4^{2-}	0.3 (4.0)	0.2 (1.7)	1.5 (13.7)	1.8 (16.6)
$PM_{2.5}$	4.5 (2.7)	0.7 (0.6)	18.1/17.5 (13.4/8.8)	23.9/18.8 (16.5/9.6)
NO_3^-/NO_y	3.2/1.1	0.6/0.5	17.9/5.9	19.5/6.3

China Plain (i.e., Beijing, Tianjin, Baoding, and Shijiazhuang; Fig. 3) where emissions of NO_x, PM, NH_3, and SO_2 are high (Streets et al., 2003; Zhang et al., 2009). Elevated emissions of NO_x and PM produced more HONO and HNO_3 through the reaction of R_{het} in both daytime and nighttime (Table 3). High emissions of NO_x further enhanced HONO through the reaction of R_{NO2S} in the daytime and direct emissions (R_{em}) in both daytime and nighttime (Table 3). Enhancements of HONO yielded more OH through the photolysis of HONO, finally producing high O_3 (Fig. 2). On the other hand, increases of OH and HNO_3 together with high emissions of NH_3 and SO_2 were favorable for the production of NO_3^-, NH_4^+, SO_4^{2-}, and $PM_{2.5}$. By contrast, areas with relatively low emissions of NO_x, PM, NH_3, and SO_2 had low percentage increases of NO_3^-, NH_4^+, SO_4^{2-}, and $PM_{2.5}$ (Fig. 3) and minor enhancements of O_3 (Fig. 2) due to minor increases of OH produced through the three additional HONO sources. In the nighttime, R_{het} produced large enhancements of NO_3^- and NH_4^+, with a maximum of ∼40% (figures not shown); however, increases of SO_4^{2-} were <9%.

The largest hourly increases in NO_3^- and NH_4^+ usually ranged from 20% to 60%. Those of SO_4^{2-} and $PM_{2.5}$ were generally between 10% and 25% over most areas of the North China Plain, except the Bohai Bay

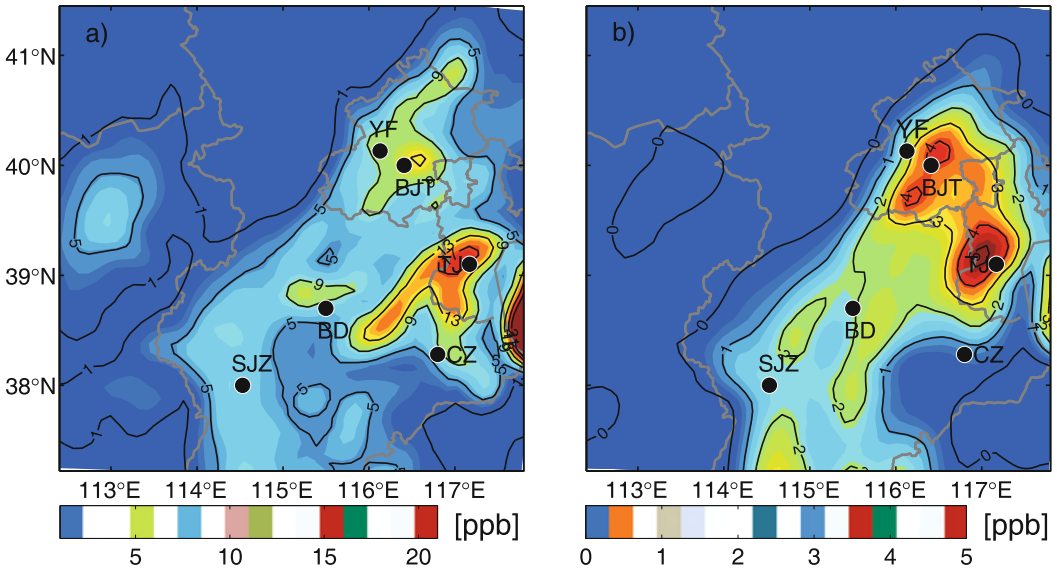

Fig. 2. Largest enhancements of (a) daily maximum 1-h O_3 and (b) monthly mean daytime (0700–1900 LST) enhancements of O_3 due to the three additional HONO sources (case E−case R) in August 2007.

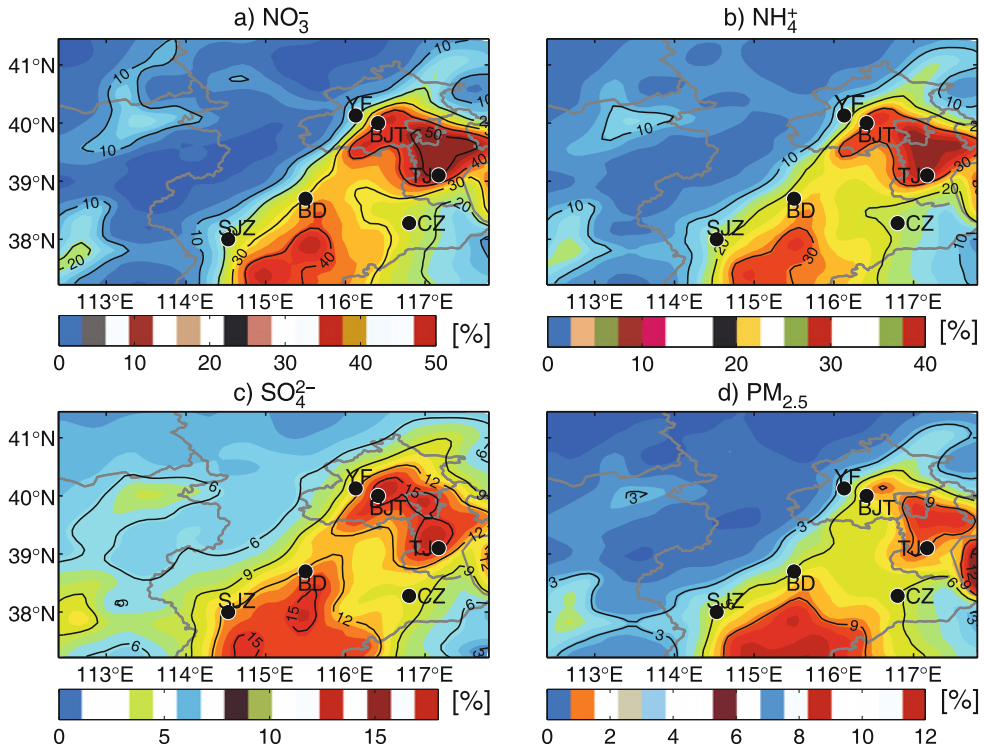

Fig. 3. Monthly mean daytime (0700–1900 LST) percentage increases of (a) NO_3^-, (b) NH_4^+, (c) SO_4^{2-}, and (d) $PM_{2.5}$ due to the three additional HONO sources in the North China Plain.

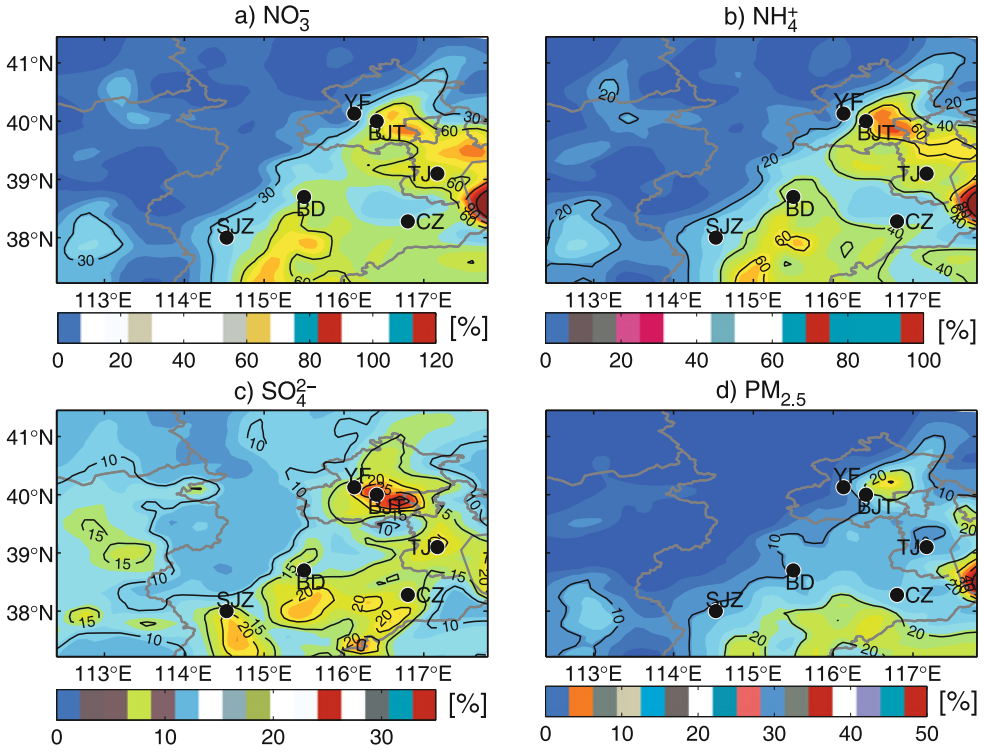

Fig. 4. Largest hourly percentage increases of (a) NO_3^-, (b) NH_4^+, (c) SO_4^{2-}, and (d) $PM_{2.5}$ due to the three additional HONO sources in the North China Plain in August 2007.

(Fig. 4). For the Bohai Bay, the largest hourly enhancements of NO_3^-, NH_4^+, and $PM_{2.5}$ >90%, 80%, and 40%, respectively (Fig. 4). Compared with inland areas of the North China Plain, the Bohai Bay has low heights of the atmospheric boundary layer (ABL) and abundant moisture (An et al., 2011). Low heights of the ABL can increase surface concentrations of air pollutants (e.g., PM and NO_x). Elevated PM concentrations and abundant moisture can enhance the aerosol surface area per unit volume through aerosol hygroscopic growth and lead to more production of HONO and HNO_3 through the reaction of R_{het}. Additionally, high NO_x concentrations and abundant moisture are favorable for R_{NO2S} which produces OH and HONO in the daytime. Large increases in HO_x (OH + HO_2) concentrations due to the additional HONO sources and high emissions of NH_3 (Streets et al., 2003) resulted in significant enhancements of NO_3^- and NH_4^+, which led to enhancements of $PM_{2.5}$ (Table 3).

3.4 *Impacts of the three additional HONO sources on* NO_{yg}/NO_y *and* NO_3^-/NO_y

For case R, high emissions of NO_x led to large monthly mean daytime concentration ratios of NO_{yg}/NO_y in major cities over the North China Plain (e.g., Beijing, Tianjin, Baoding, and Shijiazhuang, and other locations), with a maximum of 91% in Beijing (Fig. 5a). Spatial distribution of NO_{yg}/NO_y for case E is very similar to that for case R (Fig. 5b), but NO_{yg}/NO_y showed no noticeable decreases when Figs. 5a and b were compared. By contrast, large concentration ratios of NO_3^-/NO_y, with a maximum of 71%, were located in relatively low NO_x emission areas (Fig. 5c), because nitrates in the air mainly come from chemical reactions. Increases in concentration ratios of NO_3^-/NO_y were obvious when Figs. 5c and d were compared. Differences between Figs. 5a and b and between Figs. 5c and d indicate that the three additional HONO sources produced >5% of the monthly mean daytime decreases in NO_{yg}/NO_y and >5% of the monthly mean daytime increases in concentration ratios of NO_3^-/NO_y in large areas, with high emissions over the North China Plain with a maximum decrease of NO_{yg}/NO_y and a maximum increase of NO_3^-/NO_y of ~20% (Figs. 5e and f). In the nighttime, R_{het} and R_{em} led to ~3%–6% reductions in NO_{yg}/NO_y and ~3%–6% increments in NO_3^-/NO_y in large areas of the North China Plain (figures not shown). The maximum increases of NO_3^-/NO_y in the daytime were higher than those in the nighttime because R_{NO2S}, R_{het}, and R_{em} in the daytime produced greater in-

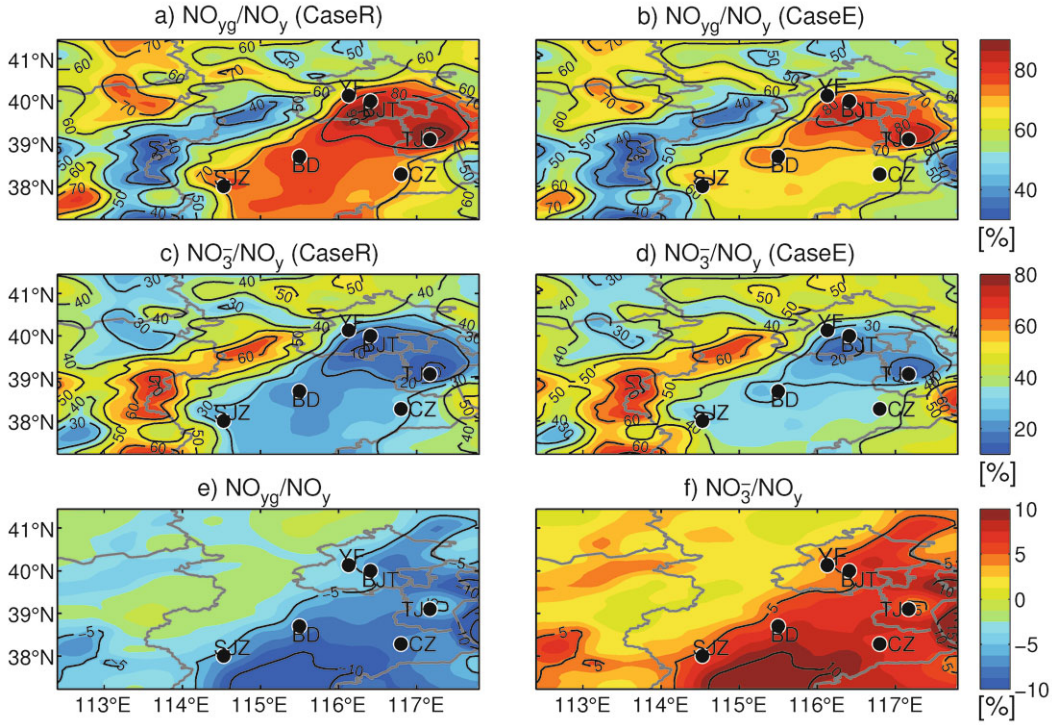

Fig. 5. Monthly mean daytime (0700–1900 LST) concentration ratios (%) of (a, b) NO_{yg} to NO_y and (c, d) NO_3^- to NO_y for cases R and E, and differences (%) in the monthly mean daytime concentration ratios of (e) NO_{yg} to NO_y and (f) NO_3^- to NO_y between cases E and R over the North China Plain in August 2007.

creases of NO_3^- than R_{het} in the nighttime (Table 3). For hourly mean concentration ratios, the largest decreases of NO_{yg}/NO_y and the maximum increases of NO_3^-/NO_y were between 15% and 52% in most areas of the North China Plain, except the Bohai Bay where the largest decreases of NO_{yg}/NO_y and the maximum increases of NO_3^-/NO_y reached 52% (figures not shown) due to low heights of the ABL and rich moisture.

Substantial increases in monthly mean concentrations, maximum hourly mean concentrations of aerosol components, particularly NO_3^- and NH_4^+, noticeable increases in monthly mean concentration ratios and the maximum hourly mean concentration ratios of NO_3^-/NO_y due to the three additional HONO sources have significant implications. High emissions of NO_x and PM produce elevated concentrations of HONO or HNO_3 through R_{em} or R_{NO2S} or R_{het}. Elevated HONO concentrations can yield more OH radicals in the daytime, leading to more formation of O_3, NO_3^-, NH_4^+, SO_4^{2-} and $PM_{2.5}$ under high emissions of NO_x, NH_3, and SO_2. At night, R_{het} and the reaction of $HNO_3 + NH_3 \rightarrow NH_4NO_3$ result in increases of NO_3^-, NH_4^+, and $PM_{2.5}$. Compared with that of gas HNO_3, NH_3, and SO_2, dry deposition velocity of NO_3^-, NH_4^+, and SO_4^{2-} is small (Zhang et al., 2004), so NO_3^-, NH_4^+, and SO_4^{2-} are favorable for long-range transport which aggravates regional air pollution. On the other hand, elevated concentrations of NO_3^-, NH_4^+, and SO_4^{2-} together with their hygroscopic growth can cause visibility impairment and enhance the incidence of haze under stagnant weather conditions.

4. Conclusions

Three additional HONO sources (i.e., R_{NO2S}, R_{het}, and R_{em}) were incorporated into WRF-Chem and five simulations were conducted over the North China Plain in August of 2007. Results show that HONO simulations were substantially improved when R_{NO2S}, R_{het}, and R_{em} were included in WRF-Chem (e.g., the root mean square error decreased by ∼50%, and the correlation coefficient improved to 0.97 from 0.19). R_{het} significantly enhance concentrations of HONO, NO_3^-, NH_4^+, and $PM_{2.5}$ in the North China Plain. The three additional HONO sources yielded significant increases in monthly mean concentrations of major aerosol components, particularly NO_3^- and NH_4^+, with a maximum of ∼50%, in major cities of the North China Plain (i.e., Beijing, Tianjin, Baoding, and Shijiazhuang). The three additional HONO sources produced ∼5%–20% increases in monthly mean concentration ratios of NO_3^-/NO_y, ∼15%–52% increases in the largest hourly mean concentration ratios of NO_3^-/NO_y, and ∼20%–60% hourly increases of NO_3^- and NH_4^+ in most areas of the North China Plain except the Bohai Bay, where largest hourly enhancements of NO_3^-, NH_4^+, and $PM_{2.5}$ >90%, 80%, and 40%, respectively. These results have important implications for atmospheric projections in that regional air pollution will be aggravated, visibility will be impaired, and the incidence of haze will be increased in some regions with elevated emissions of NO_x and PM under favorable weather conditions when the three additional HONO sources are considered.

The uncertainty of R_{het} comes mainly from the heterogeneous uptake coefficient of NO_2 (γ) and the aerosol surface area per unit volume (S_a). The γ value ranges from 10^{-6} to 10^{-3} (Jacob, 2000) and can depend on air temperature, relative humidity, and aerosol components. The modeling study conducted by Bian and Zender (2003) used a γ value of 4.4×10^{-5} for mineral dust. A value of 10^{-4} recommended by Jacob (2000) was used for considered aerosols in this research (see section 2.2). Field and laboratory experiments need to be done to reduce the uncertainty of the γ values. The uncertainty of S_a is closely related with that of emission inventories, meteorological conditions, and aerosol hygroscopic growth. For HONO emissions we have considered the suggestions of both Kurtenbach et al. (2001) and Gutzwiller et al. (2002), and we have used a reasonable expression (R_{em}, see section 2.2). The uncertainty of R_{NO2S} mainly originates from that of the rate constant for the reaction of electronically excited NO_2 with water. For this research, the mean value of 9.1×10^{-14} cm^3 molecule^{-1} s^{-1} was used (Li et al., 2011). Further experiments are required to reduce the uncertainty of the rate constant.

Acknowledgements. The research was partially supported by the National Natural Science Foundation of China (Grant Nos. 41175105 and 40905055) and the Key Project of Chinese Academy of Sciences (Grant No. kzcx1-yw-06-04). Special thanks are given to Prof. XIE Pinhua from Anhui Institute of Optics and Fine Mechanics, Chinese Academy of Sciences for providing HONO observations in Beijing, and Prof. WANG Yuesi from CERN, LAPC, Institute of Atmospheric Physics (IAP), Chinese Academy of Sciences for offering observed data of NO_x, O_3, $PM_{2.5}$, and PM_{10} at seven sites in Beijing, Tianjin, and Hebei Province. Thanks are extended to the two anonymous reviewers for key suggestions that improved the revised manuscript.

REFERENCES

An, J., W. Zhang, and Y. Qu, 2009: Impacts of a strong cold front on concentrations of HONO, HCHO, O_3, and NO_2 in the heavy traffic urban area of Beijing.

Atmos. Environ., **43**, 3454–3459.

An, J., Y. Li, F. Wang, and P. Xie, 2011: Impacts of photoexcited NO_2 chemistry and heterogeneous reactions on concentrations of O_3 and NO_y in Beijing, Tianjin and Hebei Province of China. *Air Quality-Models and Applications*, N. Mazzeo, Ed., InTech, 197–210.

Aumont, B., F. Chervier, and S. Laval, 2003: Contribution of HONO sources to the $NO_x/HO_x/O_3$ chemistry in the polluted boundary layer. *Atmos. Environ.*, **37**, 487–498.

Bian, H., and C. S. Zender, 2003: Mineral dust and global tropospheric chemistry: Relative roles of photolysis and heterogeneous uptake. *J. Geophys. Res.*, **108**(4672), doi: 10.1029/2003JD003143.

Cleemput, O. V., and A. H. Samater, 1996: Nitrite in soils: accumulation and role in the formation of gaseous N compounds. *Fertilizer Research*, **45**, 81–89.

Crowley, J. N., and S. A. Carl, 1997: OH formation in the photoexcitation of NO_2 beyond the dissociation threshold in the presence of water vapor. *J. Phys. Chem.*, **101**, 4178–4184.

Dentener, F. J., and P. J. Crutzen, 1993: Reaction of N_2O_5 on tropospheric aerosols impact on the global distributions of NO_x, O_3, and OH. *J. Geophys. Res.*, **98**(D4), 7149–7163.

Emmons, L. K., and Coauthors, 2010: Description and evaluation of the Model for Ozone and Related chemical Tracers, version 4 (MOZART-4). *Geoscientific Model Development*, **3**, 43–67.

Ensberg J. J., M. Carreras-Sospedra, and D. Dabdub, 2010: Impacts of electronically photo-excited NO_2 on air pollution in the South Coast Air Basin of California. *Atmospheric Chemistry and Physics*, **10**, 1171–1181.

Fast, J. D., W. I. Gustafson, R. C. Easter, R. A. Zaveri, J. C. Barnard, E. G. Chapman, G. A. Grell, and S. E. Peckham, 2006: Evolution of ozone, particulates, and aerosol direct radiative forcing in the vicinity of Houston using a fully coupled meteorology-chemistry-aerosol model. *J. Geophys. Res.*, **111**(D21305), doi: 10.1029/2005JD006721.

Foley, K. M., and Coauthors, 2009: Incremental testing of the community multiscale air quality (CMAQ) modeling system version 4.7. *Geoscientific Model Development,* **3**, 205–226.

Grell, G. A., S. E. Peckham, R. Schmitz, S. A. Mckeen, G. Frost, W. C. Skamarock, and B. Eder, 2005: Fully coupled "online" chemistry within the WRF model. *Atmos. Environ.*, **39**, 6957–6975.

Guenther, A., P. Zimmerman, P. C. Harley, R. K. Monson, and R. Fall, 1993: Isoprene and monoterpene emission rate variability: Model evaluations and sensitivity analyses. *J. Geophys. Res.*, **98**, 12609–12617.

Gutzwiller, L., F. Arens, U. Baltensperger, H. W. Gaggeler, and M. Ammann, 2002: Significance of semivolatile diesel exhaust organics for secondary HONO formation. *Environ. Sci. Technol.*, **36**, 677–682.

Jacob, D. J., 2000: Heterogeneous chemistry and tropospheric ozone. *Atmos. Environ.*, **34**, 2131–2159.

Kurtenbach, R., and Coauthors, 2001: Investigations of emissions and heterogeneous formation of HONO in a road traffic tunnel. *Atmos. Environ.*, **35**, 3385–3394.

Li, S., J. Matthews, and A. Sinha, 2008: Atmospheric hydroxyl radical production from electronically excited NO_2 and H_2O. *Science*, **319**, 1657–1660.

Li, G., W. Lei, M. Zavala, R. Volkamer, S. Dusanter, P. Stevens, and L. T. Molina, 2010: Impacts of HONO sources on the photochemistry in Mexico City during the MCMA-2006/MILAGO Campaign. *Atmospheric Chemistry and Physics*, **10**(14), 6551–6567.

Li, Y., J. An, M. Min, W. Zhang, F. Wang, and P. Xie, 2011: Impacts of HONO sources on the air quality in Beijing, Tianjin and Hebei Province of China. *Atmos. Environ.*, **45**(27), 4735–4744.

Qin, M., and Coauthors, 2009: An observational study of the HONO–NO_2 coupling at an urban site in Guangzhou City, South China. *Atmos. Environ.*, **43**, 5731–5742.

Sarwar, G., S. J. Roselle, R. Mathur, W. Appel, R. L. Dennis, and B. Vogel, 2008: A comparison of CMAQ HONO predictions with observations from the Northeast Oxidant and Particle Study. *Atmos. Environ.*, **42**, 5760–5770.

Sarwar, G., R. W. Pinder, K. W. Appel, R. Mathur, and A. G. Carlton, 2009: Examination of the impact of photoexcited NO_2 chemistry on regional air quality. *Atmos. Environ.*, **43**, 6383–6387.

Simpson, D., A. Guenther, C. N. Hewitt, and R. Steinbrecher, 1995: Biogenic emissions in Europe 1. Estimates and uncertainties. *J. Geophys. Res.*, **100**, 22875–22890.

Streets, D. G., and Coauthors, 2003: An inventory of gaseous and primary aerosol emissions in Asia in the year 2000. *J. Geophys. Res.*, **108**(D21), 8809, doi: 10.1029/2002JD003093.

Su, H., and Coauthors, 2008: Nitrous acid (HONO) and its daytime sources at a rural site during the 2004 PRIDE-PRD experiment in China. *J. Geophys. Res.*, **113**(D14312), doi: 10.1029/2007jd009060.

Su, H., and Coauthors, 2011: Soil nitrite as a source of atmospheric HONO and OH radicals. *Science*, **333**, 1616–1618.

Thornton, J., and J. P. D. Abbatt, 2005: Measurements of HO_2 uptake to aqueous aerosol: Mass accommodation coefficients and net reactive loss. *J. Geophys. Res.*, **110**(D08309), doi: 10.1029/2004jd005402.

Wennberg, P. O., and D. Dabdub, 2008: Rethinking ozone production. *Science*, **319**, 1624–1625.

Yu, Y., B. Galle, A. Panday A, E. Hodson, R. Prinn, and S. Wang, 2009: Observations of high rates of NO_2–HONO conversion in the nocturnal atmospheric boundary layer in Kathmandu, Nepal. *Atmospheric Chemistry and Physics*, **9**, 6401–6415.

Zaveri, R. A., R. C. Easter, J. D. Fast, and L. K. Peters, 2008: Model for Simulating Aerosol Interac-

tions and Chemistry (MOSAIC). *J. Geophys. Res.*, **113**(D13204), doi: 10.1029/2007JD008782.

Zhang, Q., and Coauthors, 2009: Asian emissions in 2006 for the NASA INTEX-B mission. *Atmospheric Chemistry and Physics*, **9**, 5131–5153.

Zhang, Y., T. Wang, Z. Hu, and C. Xu, 2004: Temporal variety and spatial distribution of dry deposition velocities of typical air pollutants over different landuse types. *Climatic and Environmental Research*, **9**(4), 591–604. (in Chinese)

Zhu, Y., W. Liu, P. Xie, K. Dou, S. Liu, F. Si, S. Li, and M. Qin, 2009: Observations of atmospheric HONO in summer of Beijing. *Environmental Science*, **30**(6), 1567–1573. (in Chinese)

Ziemba, L. D., J. E. Dibb, R. J. Griffin, C. H. Anderson, S. I. Whitlow, B. L. Lefer, B. Rappenglück, and J. Flynn, 2010: Heterogeneous conversion of nitric acid to nitrous acid on the surface of primary organic aerosol in an urban atmosphere. *Atmos. Environ.*, **44**(33), 4081–4089.